

# Analysing $J/\Psi$ Production in Various RHIC Interactions with a Version of Sequential Chain Model (SCM)

P. Guptaroy<sup>1\*</sup>, Tarun K. Garain<sup>2</sup>, Goutam Sau<sup>3†</sup>,  
S. K. Biswas<sup>4‡</sup> & S. Bhattacharyya<sup>5§</sup>

<sup>1</sup> Department of Physics, Raghunathpur College,  
Raghunathpur 723133, Purulia, West Bengal, India.

<sup>2</sup> Department of Mathematics, Raghunathpur College,  
Raghunathpur 723133, Purulia, West Bengal, India.

<sup>3</sup> Beramara Ram Chandrapur High School,  
South 24-Pgs,743609(WB),India.

<sup>4</sup> West Kodalia Adarsha Siksha Sadan, New Barrackpore,  
Kolkata-700131, India.

<sup>5</sup> Physics and Applied Mathematics Unit (PAMU),  
Indian Statistical Institute, Kolkata - 700108, India.

## Abstract

We have attempted to develop here tentatively a model for  $J/\Psi$  production in  $p+p$ ,  $d+Au$ ,  $Cu+Cu$  and  $Au+Au$  collisions at RHIC energies on the basic ansatz that the results of nucleus-nucleus collisions could be arrived at from the nucleon-nucleon ( $p+p$ )-interactions with induction of some additional specific features of high energy nuclear collisions. Based on the proposed new and somewhat unfamiliar model, we have tried (i) to capture the properties of invariant  $p_T$ -spectra for  $J/\Psi$  meson production; (ii) to study the nature of centrality dependence of the  $p_T$ -spectra; (iii) to understand the rapidity distributions; (iv) to obtain the characteristics of the average transverse momentum  $\langle p_T \rangle$  and the values of  $\langle p_T^2 \rangle$  as well and (v) to trace the nature of nuclear modification factor. The alternative approach adopted here describes the data-sets on the above-mentioned various observables in a fairly satisfactory manner. And, finally, the nature of  $J/\Psi$ -production at Large Hadron Collider(LHC)-energies deduced on the basis of our chosen model has been presented in a predictive way against the RHIC-yields, both calculated for the most central collisions and on the same model.

**Keywords:** Relativistic heavy ion collisions, inclusive production, charmed meson.

**PACS nos.:** 25.75q, 13.85Ni, 14.40Lb

---

\*e-mail: gpradeepta@rediffmail.com

†e-mail: gautamsau@yahoo.co.in

‡e-mail: sunil\_biswas2004@yahoo.com

§e-mail: bsubrata@isical.ac.in (Communicating Author).

“Finally  $J/\Psi$  suppression, which for more than 20 years has represented the gold-plated signature of deconfinement, is not understood” - M. J. Tannenbaum [1].

## 1 Introduction and Background

At the very start let us first address two somewhat imposed but important and interesting questions: (i) why are we so seriously interested in pursuing the  $\Psi$ -studies at both RHIC and LHC?; (ii) Why do we turn to a somewhat new model, leaving aside the several versions of the so-called standard model? In fact, the much-valued observation contained in and captivated by the quotation at the top from a work by Tannenbaum [1] answers, in part, simultaneously both the questions. But, an elaboration on the background and the perspective, we feel, is quite necessary for better understanding and comprehension of both the points to the desired degree and depth. Why has the  $J/\Psi$ -suppression attracted the most attention as the likely “gold-plated” signal [2]? The pioneering work of Matsui and Satz[3] established at the very beginning a few points: (i) as a hard QCD process, the heavy charm pair production takes place very easily, (ii) the Debye screening of the QGP prevents formation of a  $J/\Psi$  state in heavy ion collisions, (iii) the low temperatures at the hadronization do not really permit of the proposed charm anticharm pair kinematically; and quite soon after them, it was further proposed that the suppression pattern ought to have a characteristic transverse momentum dependence. Later, perturbative calculations based on perturbative Quantum Chromodynamics (pQCD) established the fact that both the suppression signal itself as well as its  $p_T$ -dependence could be mimicked by the mundane nuclear shadowing. It was thus quite evident from the early days that a detailed quantitative analysis would be necessary to disentangle the effects of Debye screening in QGP. It has since been recognized that other effects, notably the simple absorption of the produced  $J/\Psi$  in the nucleus, cause suppression of the produced  $J/\Psi$  in all nucleus-involved collisions, categorized physically as **normal** suppression. The additional or so-called ‘**anomalous**’ suppression as the possible signal of QGP, shall have to be investigated into only after accommodating the normal suppression. But, the estimation of these proposed normal/anomalous suppressions got absolutely entangled in multiple problems in pQCD due to lack of reliable and consistent knowledge about the several related factors. The reasons are explained quite well by Bhalerao and Gavai [2]. Besides, a detailed review made by Rapp et al.[4] has pinpointed and elucidated the several conceptual, difficulties and experimental hurdles encountered by the Standard Model

(SM) in understanding and interpreting the various aspects of the  $J/\Psi$ -data. So, in order to escape these problems and to minimise the difficulties due to uncertainties, we have tried here an alternative methodology for understanding the totality or a large of part of the data on  $J/\Psi$ -production in some ultrahigh energy collisions like  $p + p$ ,  $d + Au$ ,  $Cu + Cu$  and  $Au + Au$  interactions which comprise the totality of the contour of the experimental RHIC studies [5]-[7]. The present study aims at probing and comprehending some of the major properties and data-characteristics of  $J/\Psi$ -production in all the aforementioned RHIC-studies in a model-based manner. And the model of our choice is named to be the Sequential Chain Model (SCM) which has no QCD-tag and with some ancillary physical ideas. Very initially, and even now, the goal of high energy heavy ion physics has been to study ‘quantum chromodynamics’(QCD) in a regime of high temperature, high density and large reactive volume. The hope was and is to find conclusive evidence that ‘QCD’ undergoes a phase transition at a critical temperature from a confined state, where so-called quarks and gluons are bound in colourless hadron states, to a hypothetical deconfined state named ‘quark-gluon plasma’ (QGP), where ‘quarks’ and ‘gluons’ can explore volumes larger than the typical hadron radius ( $r \sim 1fm$ ). But in our endeavours made here we would try to avoid using all these standard phrases, propositions and methods; rather we would try to build up an entirely new and alternative approach to understand the production-mechanism for  $J/\Psi$  production and interpret the relevant observables in the light of an alternative approach outlined in the next section.

In one of our previous works [8], we demonstrated in no uncertain terms that the production of  $J/\Psi$  particles was neither ‘anomalously’ suppressed, nor enhanced; rather it was “just normal” where the term ‘normal’ is to be interpreted as the similarity of the  $J/\Psi$ -behaviour with production characteristics of some other lighter mesons and hadrons. In the past quite consciously, we never differentiated between initial state and final state effects. Herein too we do the same. And finally now we will be probing here whether there could be any special effect arising out of a smaller system-size for  $Cu + Cu$  compared to that for  $Au + Au$  reactions.

Our plan of work presented here is as follows. In the next section we try to present a model not based on the concepts of quarks and gluons; rather it is founded on altogether different facade presented in details in the Refs[9]-[12]. In section 3 we give the results and a general discussion on them. And in the last section (section 4) we offer the final remarks which essentially summarise the conclusions of this work.

## 2 The Model and the Approach

The description of the model-based features would be subdivided into two parts. The first part gives a brief overview of the  $J/\Psi$ -production mechanism in nucleon-nucleon ( $p + p$ ) interaction in the context of the Sequential Chain Model (SCM). Thereafter, the relevant transition for different observables from  $p + p$  to  $A + B$  interactions will be discussed.

The outline and characteristics of the model we use here are obtained, in the main, from one of our previous works [8]. According to this model, the photons released by two dominant varieties of vector mesons which are produced in a  $\rho$ - $\omega$ - $\pi$  sequential chain with  $\rho$  (rho) and  $\omega$  (omega) alternating with pion(s). According to this model, called Sequential Chain Model (SCM), high energy hadronic interactions boil down, essentially, to the pion-pion interactions; as the protons are conceived in this model as  $p=(\pi^+\pi^0\vartheta)$ , where  $\vartheta$  is a spectator particle needed for the dynamical generation of quantum numbers of the nucleons [9]-[16]. The particle  $\vartheta$  is called a spectator particle because it does not and cannot take part in the strong interactions, as it is identified to be a muonic neutrino and is taken to be a Majorana spinor. The internal quantum numbers like isospin, strangeness and baryon numbers can be related to the internal angular momentum of the constituents and we thus do have a geometrical origin of the basic SU(3) symmetry of the hadrons. And it is taken that these constituents move in a harmonic oscillator potential with orbital angular momentum  $1/2\hbar$  in such a way that, the two values of the third component of the orbital momentum represent the two states of matter: particles and antiparticles. The multiple production of  $J/\Psi$ -mesons in a high energy proton-proton collisions is described in the following way. The secondary  $\pi$ -meson or the exchanged  $\rho$ -meson emit a free  $\omega$ -meson and pi-meson; the pions so produced at high energies could liberate another pair of free  $\rho$  and trapped  $\omega$ -mesons (in the multiple production chain). These so-called free  $\rho$  and  $\omega$ -mesons decay quite a fast into photons and these photons decay into  $\Psi$  or  $\Psi'$  particles, which, according to this alternative approach is a bound state of  $\Omega\bar{\Omega}$  or  $\Omega'\bar{\Omega}'$  particles. The production of  $J/\Psi$ -mesons is shown schematically in Figure 1. The field theoretical calculations for the average multiplicity of the  $\Psi$ -secondaries and for the inclusive cross-sections of the psi-particles deliver some expressions which we would pick up from [8] and [17].

The inclusive cross-section of the  $\Psi$ -meson produced in the  $p + p$  collisions given by

$$E \frac{d^3\sigma}{dp^3} \Big|_{p+p \rightarrow J/\Psi+X} \cong C_{J/\Psi} \frac{1}{p_T^{N_R}} \exp\left(\frac{-5.35(p_T^2 + m_{J/\Psi}^2)}{\langle n_{J/\Psi} \rangle_{p+p}^2 (1-x)}\right) \exp(-1.923 \langle n_{J/\Psi} \rangle_{p+p} x), \quad (1)$$

where the expression for the average multiplicity for  $\Psi$ -particles in  $p + p$  scattering is

$$\langle n_{J/\Psi} \rangle_{p+p} = 4 \times 10^{-6} s^{1/4}. \quad (2)$$

In the above expression for eqn (1) the term  $|C_{J/\Psi}|$  is a normalisation parameter and is assumed here to have a value  $\cong 0.09$  for Intersecting Storage Ring(ISR)energy, and it is different for different energy region and for various collisions. The terms  $p_T$ ,  $x$  and  $m_{J/\Psi}$  represent the transverse momentum, Feynman Scaling variable and the rest mass of the  $J/\Psi$  particle respectively. Moreover, by definition,  $x = 2p_L/\sqrt{s}$  where  $p_L$  is the longitudinal momentum of the particle. The  $s$  in equation (2) is the square of the c.m. energy.

The second term in the right hand side of the equation (1), the constituent rearrangement term arises out of the partonic rearrangements inside the proton. But this proposed ‘rearrangement’ factor is different from what are implied by the terms ‘parton recombination’ or ‘parton coalescence’ in the standard literatures on  $\Psi$ -studies. In fact, this is also different from what was meant by parton rearrangement by Bleibel et al. [18]. It is established that hadrons(baryons and mesons) are composed of few partons. At large transverse momenta in the high energy interaction processes the partons undergo some dissipation losses due to the impact and impulse of the projectile on the target and the parton inside them (both the projectile and the target) they suffer some forced shifts of their placements or configurations. These rearrangements mean undesirable loss of energy, in so far as the production mechanism is concerned. The choice of  $N_R$  would depend on the following factors: (i) the specificities of the interacting projectile and target, (ii) the particularities of the secondaries emitted from a specific hadronic or nuclear interaction and (iii) the magnitudes of the momentum transfers and of a phase factor (with a maximum value of unity) in the rearrangement process in any collision. And this is a factor for which we shall have to parametrise alongwith some physics-based points indicated earlier. The parametrisation is to be done for two physical points, viz., the amount of momentum transfer and the contributions from a phase factor arising out of the rearrangement of the constituent partons. Collecting and combining all these, we proposed the relation to be given by [16]

$$N_R = 4 \langle N_{part} \rangle^{1/3} \theta, \quad (3)$$

where  $\langle N_{part} \rangle$  denotes the average number of participating nucleons and  $\theta$  values are to be obtained phenomenologically from the fits to the data-points. In this context, the only additional physical information obtained from the observations made here is: with increase in the peripherality of the collisions the values of  $\theta$  gradually grow less and less, and vice versa.

$\theta$  is a phase term related to the geometry and number of the rearrangement of the partons of the nucleus. And the number of rearrangements is constrained by the impact parameter which decides the centrality/peripherality of the collisions reflected by  $N_{part}$ .

The complex calculations of the Feynman diagram with the infinite momentum frame techniques give rise to such forms with some assumptions and approximations based on the boundedness of  $p_T$  (transverse momentum)-values. For calculation purposes we took  $f_{\rho\omega\pi}$ ,  $g_{\gamma\omega}$  and  $g_{\gamma\Psi}$  as the point-coupling of Fig.1. Moreover, in this context, we would have to reckon some other model-dependant features: (1) There are total nine probable diagrams for the various exchanges of  $\pi\pi \rightarrow \pi\pi$ . So the final contribution has a product term of  $9^2$ ; (2) Secondly, the c.m. energy of the  $\pi\pi$  system has to be translated into the actual  $p + p$  collisions for which one derives a conversion factor  $s_{\pi\pi} = \frac{4}{25}s_{pp}$ . The previous paper [9] does not contain the product term (i.e. the factor)  $1/p_T^{N_R}$ . This multiplier term has been introduced from physical considerations arising out of large- $p_T$  (hard) reactions at RHIC energies. In fact, this term has been inducted absolutely phenomenologically. But the rest is an outcome of very rigorous calculations based on ‘soft’ (small- $p_T$ ) production of particles. In nature 90% of the particles are produced with very small  $p_T$ . And our initial focus during the period 1975-1980 was to concentrate on generalized particle-production characteristics in nature.

In order to study a nuclear interaction of the type  $A + B \rightarrow Q + x$ , where  $A$  and  $B$  are projectile and target nucleus respectively, and  $Q$  is the detected particle which, in the present case, would be  $J/\Psi$ -mesons, the SCM has been adapted, on the basis of the suggested Wong [19] work to the Glauber techniques by using Wood-Saxon distributions [20]-[21]. The inclusive cross-sections for  $J/\Psi$  production in different nuclear interactions of the types  $A + B \rightarrow J/\Psi + X$  in the light of this modified Sequential Chain Model (SCM) can then be written in the following generalised form as [13]-[14]:

$$E \frac{d^3\sigma}{dp^3} |_{AB \rightarrow J/\Psi + X} = P_{J/\Psi} p_T^{-N_R} \exp(-c(p_T^2 + m_{J/\Psi}^2)) \exp(-1.923 \langle n_{J/\Psi} \rangle_{pp} x). \quad (4)$$

where  $P_{J/\Psi}$ ,  $N_R$  and  $c$  are the factors to be calculated under certain physical constraints. With the details of the calculations to be obtained from Refs.[13]-[14], the set of relations to be used for evaluating the parameters  $P_{J/\Psi}$  is given below.

$$P_{J/\Psi} = C_{J/\Psi} \frac{3}{2\pi} \frac{(A\sigma_B + B\sigma_A)}{\sigma_{AB}} \frac{1}{1 + \alpha(A^{1/3} + B^{1/3})} \quad (5)$$

Here, in the above set of equations, the third factor gives a measure of the number of wounded nucleons i.e. of the probable number of participants, wherein  $A\sigma_B$  gives the probability cross-

section of collision with ‘ $B$ ’ nucleus (target), had all the nucleons of  $A$  suffered collisions with  $B$ -target. And  $B\sigma_A$  has just the same physical meaning, with  $A$  and  $B$  replaced. Furthermore,  $\sigma_A$  is the nucleon(proton)-nucleus(A) interaction cross section,  $\sigma_B$  is the inelastic nucleon(proton)-nucleus(B) reaction cross section and  $\sigma_{AB}$  is the inelastic  $AB$  cross section for the collision of nucleus  $A$  and nucleus  $B$ . The values of  $\sigma_{AB}$ ,  $\sigma_A$ ,  $\sigma_B$  are worked here out in a somewhat heuristic manner by the following formula [22]

$$\sigma_{AB}^{inel} = \sigma_0 (A_{projectile}^{1/3} + A_{target}^{1/3} - \delta)^2 \quad (6)$$

with  $\sigma_0 = 68.8$  mb,  $\delta = 1.32$ .

Besides, in expression (5), the fourth term is a physical factor related with energy degradation of the secondaries due to multiple collision effects. The parameter  $\alpha$  occurring in eqn.(5) above is a measure of the fraction of the nucleons that suffer energy loss. The maximum value of  $\alpha$  is unity, while all the nucleons suffer energy loss. This  $\alpha$  parameter is usually to be chosen [19], depending on the centrality of the collisions and the nature of the secondaries.

The “ $P_{J/\Psi}$ ” factor in the expression (5) accommodates a wide range of variation because of the existence of the large differences in the in the normalizations of the  $J/\Psi$  cross-sections for different types of interactions. The constraints for calculating  $P_{J/\Psi}$  are mentioned above.

The parameter ‘ $N_R$ ’ of Eqn. (4) has been calculated from the Eqn.(3). The constraints for calculating  $N_R$  have been stated in the paragraph written below the Eqn. (4).

The parameter ‘ $c$ ’ is a energy and rapidity dependent term. It is clear from eqn. (1) that energy dependent factor comes from the average multiplicity of  $J/\Psi$  particles ( $\sim s^{-0.125}$ ) and the rapidity factor comes from  $(1-x)$  where  $x = \frac{2m_T \sinh y_{cm}}{\sqrt{s}}$ . So,  $c$  has different values for different energies and rapidity regions.

The parameters used in this work are (i)  $C_{J/\Psi}$  is a normalization term which is by nature species-dependent and energy-dependent; (ii)  $N_R = 4 < N_{part} >^{1/3} \theta$ ; this is determined by fits to the invariant cross-section data. It is naturally found to be both secondary-species and centrality-dependent; (iii) Finally,  $\alpha$  is the fraction of the nucleus that suffer energy by undergoing multiple collisions and this  $\alpha$ -factor too has weak centrality dependence.

The parameters are generally obtained from the minimization of  $\chi^2$  of the experimental spectrum for invariant cross-section which involves some rigorous statistical methods and complications. But the main issues on parameter-constraining are the following few points: (i) availability of the large number of experimental data-points; (ii) smallness of the uncertainty-ranges in the

measured data. Unfortunately, for  $J/\Psi$  production, in any high energy collision whatsoever, the number of data points are relatively sparse, especially for the large transverse momentum values. Secondly, the uncertainty ranges in the measurements are also quite considerable, for which we completely dropped the idea and bid to devise the methods of constraining the evolved parameters. Very recently, Arleo and d'Enterria [23] studied on constraining the parameters for very simple and abundantly produced neutral pion production in  $pp$ -scattering at  $\sqrt{s}=22.4$  GeV and ended up with a statement like “ At high  $p_T$ 's the fit is completely unconstrained due to the lack of data, and its uncertainty is very large.”

### 3 Model-based Analyses and the Results

Here, what we need to emphasize is that the observables are different at the same energy. So let us split up the cases and treat the data available on them, individually and on a case to case basis.

#### 3.1 $J/\Psi$ (total) Crosssections in $p + p$ Interactions

As the psi-productions are generically treated rightly as the resonance particles, the standard practice is to express the measured  $J/\Psi$  (total) crosssections times branching ratio to muon or electrons, i.e.for lepton pairs , that is by  $B_W \sigma_{p+p}^{J/\Psi}$  [24]. And this is usually done for all the symmetric nuclear collision like  $Au + Au$ ,  $Pb + Pb$  and  $Cu + Cu$  etc.

By using expression (4) we arrive at the expressions for the differential cross-sections for the production of  $J/\Psi$ -mesons in the mid and forward-rapidities (i.e.  $|y| < 0.35$  and  $1.2 < |y| < 2.2$  respectively) in  $p + p$  collisions at  $\sqrt{s_{NN}}=200$  GeV at RHIC.

$$\frac{1}{2\pi p_T} B_W \frac{d^2\sigma}{dp_T dy} \Big|_{p+p \rightarrow J/\Psi+X} = 6.1 p_T^{-1.183} \exp[-0.13(p_T^2 + 9.61)] \quad \text{for } |y| < 0.35, \quad (7)$$

and

$$\frac{1}{2\pi p_T} B_W \frac{d^2\sigma}{dp_T dy} \Big|_{p+p \rightarrow J/\Psi+X} = 6.5 p_T^{-1.183} \exp[-0.16(p_T^2 + 9.61)] \quad \text{for } 1.2 < |y| < 2.2. \quad (8)$$

For deriving the expressions (7) and (8) we have used the relation  $x \simeq \frac{2p_{Tcm}}{\sqrt{s}} = \frac{2m_T \sinh y_{cm}}{\sqrt{s}}$  [25], where  $m_T$ ,  $y_{cm}$  are the transverse mass of the produced particles and the rapidity distributions.  $m_{J/\Psi} \simeq 3096.9 \pm 0.011 MeV$  [25] and  $B_W$ , the branching ratio is for muons or electrons i.e. its for lepton pairs  $J/\Psi \rightarrow \mu^+ \mu^- / e^+ e^-$ , is taken as  $5.93 \pm 0.10 \times 10^{-2}$  [25] in calculating the above equations.



Table 1: Values of  $b_{J/\Psi}$  and  $N_R$  for different centrality regions in  $Cu + Cu$  collisions

Centrality [ $ y  < 0.35$ ]	0-20%	20-40%	40-60%	60-92%
$b_{J/\Psi}$	$6.40 \times 10^{-5}$	$3.82 \times 10^{-5}$	$1.22 \times 10^{-5}$	$2.10 \times 10^{-6}$
$N_R$	0.829	0.709	0.625	0.615
Centrality [ $1.2 <  y  < 2.2$ ]	0-20%	20-40%	40-60%	60-92%
$b_{J/\Psi}$	$6.38 \times 10^{-5}$	$2.82 \times 10^{-5}$	$0.82 \times 10^{-5}$	$1.90 \times 10^{-5}$
$N_R$	0.829	0.709	0.625	0.615

In Figure (2), we have drawn the solid lines depicting the model-based results with the help of above two equations (7) and (8) against the experimental measurements [26],[27].

### 3.2 Invariant yields of $J/\Psi$ Particles in $d + Au$ , $Cu + Cu$ and $Au + Au$ Collisions

From the expression (4), we arrive at the invariant yields for the  $J/\Psi$ -production in  $d + Au \rightarrow J/\Psi + X$  reactions for mid and forward-rapidities.

$$\frac{1}{2\pi p_T} \frac{d^2 N}{dp_T dy} \Big|_{d+Au \rightarrow J/\Psi+X} = 7.25 \times 10^{-7} p_T^{-0.629} \exp[-0.13(p_T^2 + 9.61)] \quad \text{for } |y| < 0.35, \quad (9)$$

and

$$\frac{1}{2\pi p_T} \frac{d^2 N}{dp_T dy} \Big|_{d+Au \rightarrow J/\Psi+X} = 4.25 \times 10^{-7} p_T^{-0.629} \exp[-0.16(p_T^2 + 9.61)] \quad \text{for } 1.2 < |y| < 2.2. \quad (10)$$

In Figure (3), we have drawn the solid lines depicting the model-based results with the help of above two equations (9) and (10) against the experimental measurements [28].

For the case of  $Cu+Cu$  collisions at RHIC, the values of  $b_{J/\Psi} = P_{J/\Psi} \times \exp(-1.923 < n_{J/\Psi} >_{pp} x)$ <sup>1</sup> and  $N_R$  of expression (4) are given in Table 1 for the rapidities  $|y| < 0.35$  and  $1.2 < |y| < 2.2$  respectively and they are plotted in Figure 3. The exponential parts for different rapidities are remain the same as in equation (7) and equation (8). As previously stated, the exponents  $N_R$  of  $p_T$  depend on the following three factors mentioned in the previous section. The values of  $< N_{part} >$  of equation (3) for different centralities of  $Cu + Cu$  collisions have been taken from [29] and the calculations have been done accordingly. The experimental results for the invariant yields of  $J/\Psi$  production as a function of transverse momenta [30] at different centrality values

<sup>1</sup>The exponential part, here, contains  $s$  and  $x$  i.e. the squared c.m. energy and the rapidity factor  $y_{cm}$ . This, in course of calculations, gives some fixed values and is multiplied with  $P_{J/\Psi}$  to give the final product  $b_{J/\Psi}$ .

Table 2: Values of  $b_{J/\Psi}$  and  $N_R$  for different centrality regions in  $Au + Au$  collisions

Centrality [ $ y  < 0.35$ ]	0-20%	20-40%	40-60%	60-92%
$b_{J/\Psi}$	$1.32 \times 10^{-3}$	$0.86 \times 10^{-3}$	$1.65 \times 10^{-4}$	$0.25 \times 10^{-5}$
$N_R$	1.023	0.954	0.834	0.732
Centrality [ $1.2 <  y  < 2.2$ ]	0-20%	20-40%	40-60%	60-92%
$b_{J/\Psi}$	$0.91 \times 10^{-3}$	$0.42 \times 10^{-3}$	$0.19 \times 10^{-3}$	$0.22 \times 10^{-4}$
$N_R$	1.023	0.954	0.834	0.732

ranging from 0 – 20% to 60 – 92% are plotted in Fig. (4). The solid lines in the figures show the model-based results.

Similarly, for  $Au + Au$  collisions at  $\sqrt{s_{NN}}=200$  GeV at RHIC, the values of  $b_{J/\Psi}$  and  $N_R$  of equation (4) for different centrality regions are shown in Table 2 and the model-based results are plotted in Fig.5. For calculating the values of  $N_R$ , we have used the values of  $\langle N_{part} \rangle$  from [31]. The experimental results for the invariant yields of  $J/\Psi$  production as a function of transverse momenta at different centrality values ranging from 0 – 20% to 60 – 92% and for the rapidities  $|y| < 0.35$  and  $1.2 < |y| < 2.2$  respectively are taken from the PHENIX Collaboration [31].

### 3.3 Rapidity Distributions for Different reactions at $\sqrt{s_{NN}} = 200 GeV$

For the calculation of the rapidity distribution from the set of equations (1), (2), (3) and (4) we can make use of a standard relation as given below:

$$\frac{dN}{dy} = \int \frac{1}{2\pi p_T} \frac{d^2N}{dp_T dy} dp_T \quad (11)$$

The rapidity distributions for the  $J/\Psi$ -production has now been reduced to a simple relation stated hereunder

$$\frac{dN}{dy} = a_1 \exp(-0.23 \sinh y_{cm}). \quad (12)$$

The normalization factor  $a_1$  depends on the centrality of the collisions and is obvious from the nature of the eqn.(1), eqn. (2), eqn.(3) eqn.(4) and eqn. (11).

For  $p + p$  and  $d + Au$  collisions, the calculated rapidity distribution equations are

$$\frac{dN}{dy} |_{p+p \rightarrow J/\Psi+X} = 1.215 \times 10^{-6} \exp(-0.23 \sinh y_{cm}), \quad (13)$$

Table 3: Values of  $a_1 \times 10^{-6}$  for different centrality regions for  $Au + Au$  collisions

Centrality	0-20%	20-40%	40-60%	60-92%
$a_1$	0.472	0.033	0.011	0.002

and

$$\frac{dN}{dy} \Big|_{d+Au \rightarrow J/\Psi+X} = 7.025 \times 10^{-6} \exp(-0.23 \sinh y_{cm}), \quad (14)$$

In Fig. 6 and Fig. 7 we have plotted the rapidity distributions for  $J/\Psi$ -production in  $p + p$  and  $d + Au$  collisions respectively. Data in those figures are taken from Ref. [28] and the lines show the theoretical outputs.

To calculate the rapidity distribution for  $Au + Au$  collisions we are taking into account the different centrality regions by making use of Table 2 in addition to Eqs. (4) and (11). The values of  $a_1$  are different for different centrality regions for  $Au + Au$  collisions and they are given in the Table 3.

The solid lines in the Fig. 8 depict the theoretical plots of  $dN/dy$  vs.  $y$  for different centralities while the data for  $Au + Au$  collisions are taken from Ref.[30].

### 3.4 $\langle p_T \rangle$ and $\langle p_T^2 \rangle$ Values

Next we attempt at deriving model-based expressions for both  $\langle p_T \rangle$  and  $\langle p_T^2 \rangle$ . Of these twin observables the  $\langle p_T \rangle$  would be used by us in obtaining the ratios  $R_{AA}$ -s for different participant numbers,  $N_{part}$ . Though, very strangely, there is so far no data on  $\langle p_T \rangle^{J/\Psi}$  even for  $p + p$  collisions at ISR to RHIC, we have chosen here to calculate and plot the nature of  $\langle p_T \rangle^{J/\Psi}$  vs.  $N_{part}$  for some collisions under study here for the following reasons: (i) in our opinion,  $\langle p_T \rangle^{J/\Psi}$  is more fundamental observable than  $\langle p_T \rangle^2$ , (ii) for cases of almost all the secondaries produced in high energy collisions it is found that  $\langle p_T \rangle \neq \langle p_T^2 \rangle$  or  $\langle p_T \rangle^2 \neq \langle p_T^2 \rangle$  and (iii) we find in our work that  $J/\Psi$  behaves quite similarly as many other hadronic secondaries in nearly all the high energy interactions. So, plots of  $\langle p_T \rangle$  vs.  $N_{part}$  for  $Cu + Cu$  and  $Au + Au$  collisions are shown in Fig. 9 mostly in a predictive vein with the hope that it would be measured in future. And the excessive importance given to  $\langle p_T \rangle^{J/\Psi}$  here by both the theorists and the experimentalists is just contextual. But, from physical

considerations, one must admit,  $\langle p_T \rangle$  is much more important than  $\langle p_T^2 \rangle$ . Furthermore, we also uphold the view that the theorists should not be guided by just the situational constructs of the experimentalists.

The definition for average transverse momentum  $\langle p_T \rangle^{J/\Psi}$  is given below.

$$\langle p_T \rangle^Q = \frac{\int_{p_T(min)}^{p_T(max)} p_T E \frac{d^3\sigma^Q}{dp^3} dp_T^2}{\int_{p_T(min)}^{p_T(max)} E \frac{d^3\sigma^Q}{dp^3} dp_T^2}, \quad (15)$$

The theoretical plot of the average transverse momentum  $\langle p_T \rangle^{J/\Psi}$  in  $Cu + Cu$  and  $Au + Au$  collisions at RHIC for different number of participating nucleons is shown in the Fig.9. The theoretical calculations are done on the basis of uses of eqn.(4), Table 1 and Table 2.

The QCD-oriented models believe that the transverse momentum distributions of the produced  $J/\Psi$ s carry valuable information about the mechanism for their absorption or disappearance manifested in the clearly falling nature of the production cross-section. The ideas based on the Standard Model (SM) predict that there should be a decrease of  $\langle p_T^2 \rangle$  with centrality for sufficiently central collisions which is viewed as a consequence of the colour deconfinement ‘turnover effect’[32], [33]. The present model-dependent behaviour of the observables  $\langle p_T^2 \rangle$  as is defined by the undernoted relation (eqn. 16 given below). The  $[\langle p_T^2 \rangle]$  is measured by RHIC and other experiments which is supposed to have a close relationship with what-is-called-to-be the “ $J/\Psi$  suppression”, according to the QCD-points of view and to some QCD-oriented models.

The expression for the average of the squared transverse momenta for any secondary ( $Q$ ), by definition, is

$$\langle p_T^2 \rangle^Q = \frac{\int_{p_T(min)}^{p_T(max)} p_T^2 E \frac{d^3\sigma^Q}{dp^3} dp_T^2}{\int_{p_T(min)}^{p_T(max)} E \frac{d^3\sigma^Q}{dp^3} dp_T^2}, \quad (16)$$

Using the above definition and putting the form of inclusive cross-section given by eqn.(4) into use, we calculate the  $\langle p_T^2 \rangle$  for the  $J/\Psi$  production in  $d + Au$ ,  $Cu + Cu$  and  $Au + Au$  collisions at RHIC energy  $\sqrt{s_{NN}} = 200$  GeV . The values of  $p_T(min)$  and  $p_T(max)$  are taken here 0 and 5 respectively [28], [30], [31].

We are interested not only in the absolute values of  $\langle p_T^2 \rangle$  alone, but also in the centrality-dependence of them. Because, the conventional view holds the idea that  $\langle p_T^2 \rangle$  has a specific form of centrality-dependence, for which we present the graphical representations of  $N_{part}$  dependence of  $\langle p_T^2 \rangle$  for the rapidities  $|y| < 0.35$  and  $1.2 < |y| < 2.2$  and for  $d + Au$ ,  $Cu + Cu$

Table 4: Comparison of  $\langle p_T^2 \rangle$  values:: SCM vs. Hydro+ $J/\Psi$  [36] for different centrality bins and in mid-rapidity region in  $p+p$  and  $Au+Au$  collisions against the background of experimental values.

Reactions	Centrality	$N_{part}$	$\langle p_T^2 \rangle$ ( $[GeV/c]^2$ ) (Expt.)	$\langle p_T^2 \rangle$ ( $[GeV/c]^2$ ) (SCM)	$\langle p_T^2 \rangle$ ( $[GeV/c]^2$ ) (Hydro+ $J/\Psi$ )
$p + p$		2	$4.1 \pm 0.2 \pm 0.1$	3.65	3.87
$Au + Au$	0 – 20%	280	$3.6 \pm 0.6 \pm 0.1$	3.64	3.76
	20 – 40%	140	$4.6 \pm 0.5 \pm 0.1$	3.66	3.80
	40 – 60%	60	$4.5 \pm 0.7 \pm 0.2$	3.55	3.81
	60 – 92%	14	$3.6 \pm 0.9 \pm 0.2$	3.43	3.81

and  $Au + Au$  collisions in Figures 10 (a) and (b) respectively. The experimental values are taken respectively from [28], [30], [31].

Moreover, in Table 4, we present  $\langle p_T^2 \rangle$  calculated from the two theoretical models, the SCM and the ‘Hydro+ $J/\Psi$ ’ [36], with the experimental values [30] for  $p + p$  and  $Au + Au$  collisions at RHIC energies.

### 3.5 The Nuclear Modification Factor $R_{AA}$

There is yet another very important observable called nuclear modification factor (NMF), denoted here by  $R_{AA}$  which for the production of  $J/\Psi$  is defined by [30]

$$R_{AA} = \frac{d^2 N_{J/\Psi}^{AA}/dp_T dy}{\langle N_{coll}(b) \rangle d^2 N_{J/\Psi}^{pp}/dp_T dy}. \quad (17)$$

the SCM-based results on NMFs for  $Cu + Cu$  and  $Au + Au$  collisions are deduced on the basis of Eqn.(4), Eqn.(7), Eqn.(8) and Table 1 ,Table 2 and they are given by the undernoted relations

$$R_{AA}|_{Cu+Cu \rightarrow J/\Psi+X} = 0.42 p_T^{0.35} \quad for \quad |y| < 0.35, \quad (18)$$

$$R_{AA}|_{Cu+Cu \rightarrow J/\Psi+X} = 0.38 p_T^{0.35}, \quad for \quad 1.2 < |y| < 2.2. \quad (19)$$

and

$$R_{AA}|_{Au+Au \rightarrow J/\Psi+X} = 0.36 p_T^{0.16} \quad for \quad |y| < 0.35, \quad (20)$$

$$R_{AA}|_{Au+Au \rightarrow J/\Psi+X} = 0.26p_T^{0.16}, \quad for \quad 1.2 < |y| < 2.2. \quad (21)$$

wherein the value of  $\langle N_{coll}(b) \rangle$  to be used is  $\approx 170.5 \pm 11$  [34] for  $Cu + Cu$  collisions and for  $Au + Au$  collisions it is taken as  $\approx 955.4 \pm 93.6$  [35]. In Fig. 11, we plot  $R_{AA}$  vs.  $p_T$  for 0 – 20% central region in  $Cu + Cu$  and  $Au + Au$  collisions. The solid lines in the figure show the SCM-based results against the experimental results [30], [31].

Next, for the analysis of centrality dependence as represented by ( $N_{part}$ ), of the nuclear modification factor, ( $R_{AA}$ ) for  $Cu + Cu$  and  $Au + Au$  collisions at RHIC, we proceed in the direction with the help of eqn.(3), (4) and the calculated  $\langle p_T \rangle$ s [Fig.5] for forward rapidity and different centralities. For  $Cu + Cu$  collisions, the data in Figure 12 are taken from [30]. The solid line in that figure gives the SCM-based results. The dotted lines in Figure 12 show the hydrodynamical (‘Hydro+ $J/\Psi$ ’) model-based calculations with and without nuclear absorption (‘hydro+j/Psi 1’ and ‘hydro+J/Psi 2’ respectively) [37]. And for the  $Au + Au$  collisions, the data in Figures 13(a) and (b) are taken from [31],[38]. The solid line in that figure gives the SCM-based results against the background of some other predictions or calculations [38], [39] [37].

### 3.6 LHC Prediction

On the basis of the model-based calculations shown above, we now make the prediction for the invariant yields of  $J/\Psi$ -mesons in the most central (0-10%)  $Pb + Pb$ -collisions at the  $\sqrt{s_{NN}} = 5500$  GeV i.e. at Large Hadron Collider (LHC) energy. The equation of the invariant yields of  $J/\Psi$  in the reaction of the type  $Pb + Pb \rightarrow J/\Psi + X$  for the forward rapidity region would be of the form as given below

$$\frac{1}{2\pi p_T} B_W \frac{d^2 N}{dp_T dy} |_{Pb+Pb \rightarrow J/\Psi+X} = 0.53 \times 10^{-2} p_T^{-1.123} \exp[-0.069(p_T^2 + 9.61)] \quad for \quad 1.2 < |y| < 2.2. \quad (22)$$

In Figure 14, we had presented the predicted nature of the yields for  $J/\Psi$  production in  $Pb + Pb$  collisions at LHC-energy by the solid curve. The dashed plot in the figure represents our RHIC calculations based on eqn.(4) and Table 2 in sect. 3.2.

## 4 Summary and Conclusions

In assessing the results achieved we must remember the limitations of the circumstances and the issues. It has to be appreciated that psions ( $J/\Psi$ -mesons) are not as abundant as pions, the

commonest variety of the secondaries. the cross-sections for  $J/\Psi$ -production fall a few orders of magnitude compared to the pions. Besides, the uncertainties in the measurements of these psi-particles (resonance) are also much larger. So, in seeking the agreements of the model-based results with the measured data on  $J/\Psi$ -particles, one must be realistic. No model could probably claim a cent-percent agreement with data under such circumstances as pointed out above. For this reason, we have frequently compared here our model-based results with both the experimental data and the results obtained by one or two other competing models. There is yet another point very specific to  $J/\Psi$ -particles. The number of available and reliable data on psi-production in most cases is too limited. So, we will have to cut down our expectations about the degree of convergence between the calculations and the data and to arrive at the justified comments on any model-based work on  $J/\Psi$ . On this basis, we point out the following set of observations on the present work. (i) The agreement between our model-based (SCM-based) calculations and the  $p_T$ -dependence of the invariant cross-sections on production  $J/\Psi$ -particles is modestly satisfactory, for mid and forward rapidities, moderate- $p_T$  and central nuclear collisions, though there are some degrees of discrepancies for the other regions. This statement is valid on an overall basis for the figures from Fig.2 – Fig.5. (ii) The plots on studies of rapidity dependence are somewhat constrained by the very sparse data sets, for which we could make no strong or emphatic comment about the nature of agreements or disagreements. And this is a comment valid for the figures presented in Fig. 6 to Fig. 8. (iii) We discussed in the text given above somewhat extensively on the implications of the  $\langle p_T^2 \rangle^{J/\Psi}$  and  $\langle p_T \rangle^{J/\Psi}$ -plots; our results, based on the Figs. (9) and (10) and indicated by the Table-4 show fairly good agreement for  $\langle p_T^2 \rangle^{J/\Psi}$ -data obtained by nuclear collisions and also with ‘Hydro+ $J/\Psi$ ’ model [36]. (iv) And the results shown by Fig.(11)- Fig.(13) present a comprehensive study on the measured observable  $R_{AA}$  and the model-based results, including the SCM-based plots in solid lines. (v) The Fig. 14 depicts our SCM-based predictions for the behaviour of the observable at LHC energy and in the LHC experiments at CERN.

Thus, finally, we end up with a few conclusive remarks about the physical significance of the work: (i) As the standard model does not appear to be too promising for  $J/\Psi$ -production behaviour, we have reasonably attempted a new one, surely with a certain degree of tentativeness. (ii) Neither the measurements for  $Cu + Cu$  interactions, nor the findings for  $Au + Au$  reactions at RHIC energies provide any final affirmation or clear indication of the QGP Physics. This is what is established by the very recent studies of both Tanenbaum [1],and Bhalerao, Gavai

[2]. (iv) The underlying mechanism that has been used here is not based on any ‘gluonisation’-concepts; so this approach remains value-neutral to such theoretical inductions. (v) Nor does this mechanism view the  $J/\Psi$  particles as the products of the heavy quarks, for which the ideas of ‘heavy quarks’ cannot be accommodated in this model; Similarly the phrases like ‘quark-gluon plasma’ (QGP), ‘anomalous suppression’ etc. find no place in our work. (vi) But, the new mechanism for  $J/\Psi$ -production suggested by us, here incorporates the features of ‘normal’ suppression by the inclusion of the physical term of ‘partonic rearrangement factor’ yielding the normal suppression effect arising out mainly only at large transverse momentum values belonging to ‘hard’- $p_T$  reactions. (vii) And for the ‘hard’ sector of hadronic collisions this model takes, without any exception, into account this ‘constituent (or partonic) rearrangement factor’ for production of all the secondaries (light or heavy) in a consistent manner, though certainly not on a uniform rate, which is certainly secondary-specific in nature. Thus, the ‘globality property’ of particle production at high energy (and at large  $p_T$ ) is upheld for the production of even  $J/\Psi$ -mesons and so is not to be treated on a different basis in our approach. (viii) The anomalous observations [40] on the centrality dependence of the rapidity distributions very recently taken serious note of are kept consciously out of the purview of the present work and would be dealt with in a future work.



## References

- [1] M. J. Tanenbaum, arXiv:0811.0532 v1 [nucl-ex] 04 Nov. 2008.
- [2] R. S. Bhalerao and R. V. Gavai, arXiv:0812.1619 v1 [nucl-ex] 09 Dec. 2008.
- [3] T. Matsui and H.Satz, Phys. Lett B**178**, 416 (1986).
- [4] R. Rapp, D. Blaschke and P. Crochet, arXiv:0807.2470 v2 [hep-ph] 02 Jan. 2009.
- [5] L. Bravina et al., arXiv:0811.0790 v1 [nucl-ex] 05 Nov. 2008.
- [6] E. G. Ferreira, F. Fleuret, J. P. Lansberg, A. Rakotozafindrabe, arXiv:0809.4684 v1[hep-ph] 26 Sep. 2008.
- [7] D. Kharzeev, E. Levin, M. Nardi, K. Tuchin, arXiv:0809.2933 v1[hep-ph] 17 Sep. 2008.
- [8] P. Guptaroy, Bhaskar De, G. Sanyal, S. Bhattacharyya, Int. J. Mod. Phys. A**20**, 5037 (2005).
- [9] P. Bandyopadhyay, R. K. Roychoudhury, S. Bhattachayya and D. P. Bhattacharyya, IL Nuovo Cimento A **50**, 133 (1979).
- [10] S. Bhattacharyya and P. Pal, IL Nuovo Cimento C**9**,961 (1986).
- [11] S. Bhattacharyya, IL Nuovo Cimento C**11**, 51 (1988).
- [12] S. Bhattacharyya, J. Phys. G**14**, 9 (1988).
- [13] P. Guptaroy, Bhaskar De, S. Bhattacharyya, D. P. Bhattacharyya, Int. J. Mod. Phys. E**12**,493 (2003).
- [14] P. Guptaroy, Bhaskar De, S. Bhattacharyya, Heavy Ion Physics **17**,167 (2003).
- [15] P. Guptaroy, Bhaskar De, Goutam Sau, S. K. Biswas, S. Bhattacharyya, Int. J. Mod.Phys. A **22**, 5121 (2007).
- [16] P. Guptaroy, Goutam Sau, S. K. Biswas, S. Bhattacharyya, Mod.Phys. Lett. A**23**, 1031 (2008).
- [17] G. Sanyal, Ph.D. Thesis, Calcutta University (1979).
- [18] J. Bleibel , G. Bureau and C. Fuchs Phys Lett B**659**,520 (2008).
- [19] C. Y. Wong:‘Introduction to High-Energy Heavy Ion Collisions’ (World Scientific,1994).
- [20] K. J. Eskola, P. V. Ruuskanen and K. Tuominen, Phys. Lett. B **543**, 208 (2002).
- [21] M.I. Gorenstein, A. P. Kostyuk, H. Stöcker and W. Greiner, Phys. Lett. B **524**, 264 (2002).
- [22] M.C.Abreu et al, NA50 Collaboration, Preprint, CERN-EP/2002-017(Feb. 15, 2002).
- [23] F. Arleo and D. d’Enterria arXiv:0807.1252 v2 [hep-ph], 07 Nov. 2008.
- [24] M. Gonin, NA50 Collaboration, Proc. of the ‘Physics and Astrophysics of Quark-Gluon Plasma’ ed. by Sinha et al., Narosa Pub.House (1998) p 393.
- [25] W.-M. Yao et al., Particle Data Group, J. Phys. G**33**, 1, (2006).

- [26] A. Adare et al., PHENIX Collaboration, Phys. Rev. Lett. **98**, 232002, (2007).
- [27] M. J. Leitch, J. Phys. G **34**, S453, (2007).
- [28] A. Adare et al., PHENIX Collaboration, Phys. Rev. C **77**, 024912, (2008).
- [29] B. Alver et al., PHOBOS Collaboration, arXiv:0802.1695v1 [nucl-ex], 12 Feb 2008.
- [30] A. Adare et al., PHENIX Collaboration, Phys. Rev. Lett. **101**, 122301, (2008).
- [31] A. Adare et al., PHENIX Collaboration, Phys. Rev. Lett. **98**, 232301, (2007).
- [32] D. Kharzeev, Proc. of the ‘Physics and Astrophysics of Quark-Gluon Plasma’ ed. by Sinha et al., Narosa Pub. House (1998) p 407.
- [33] D. Kharzeev, M. Nardi, H. Satz, Phys. Lett. **B405**, 14 (1997).
- [34] B. Alver et al., PHOBOS Collaboration, Phys. Rev. Lett. **96**, 212301, (2006).
- [35] S. S. Adler et al., PHENIX Collaboration, Phys. Rev. C **69**, 034909, (2004).
- [36] A.K. Chaudhuri, arXiv:0808.2702 v2 [nucl-th] 24 Nov. 2008.
- [37] A.K. Chaudhuri, J. Phys. G **35**, 095107 (2008).
- [38] Xingbo Zhao and Ralf Rapp, arXiv:0712.2407v1 [hep-ph], 14 Dec. 2007.
- [39] I. Vitev, Phys. Lett **B639**, 38 (2006).
- [40] D. Prorok, L. Turko and D. Blaschke arXiv:0901.0166v1 [hep-ph], 01 Jan. 2009.

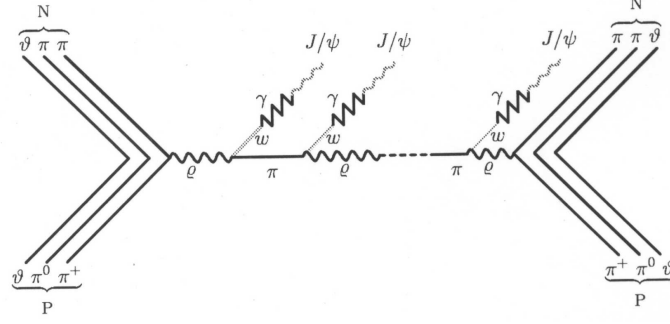


Figure 1: Schematic diagram of multiple production of  $J/\Psi$  particles in  $p+p$  scattering in the Sequential Chain Model.

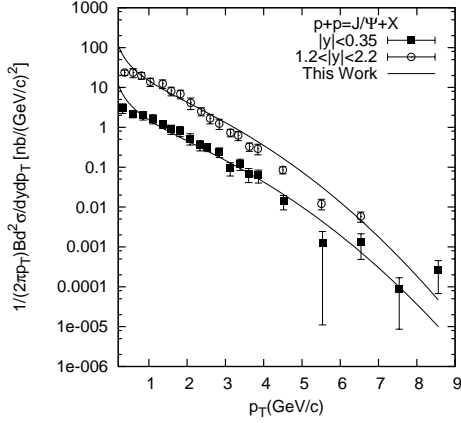


Figure 2: Plot of the invariant cross-section for  $J/\Psi$  production in proton-proton collisions at  $\sqrt{s_{NN}} = 200 \text{ GeV}$  as function of  $p_T$ . The data points are from [26]. The solid curves show the SCM-based results.

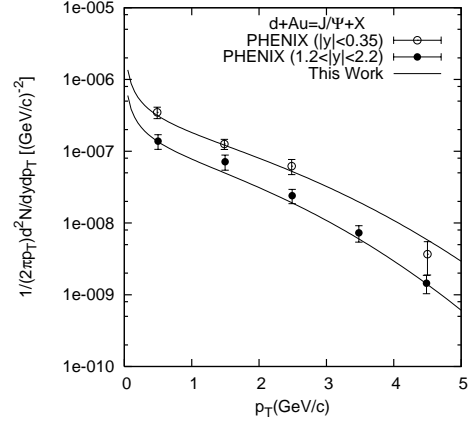


Figure 3: Plot of the invariant cross-section for  $J/\Psi$  production in  $d + Au$  collisions at  $\sqrt{s_{NN}} = 200 \text{ GeV}$  as function of  $p_T$ . The data points are from [28]. The solid curves show the SCM-based results.

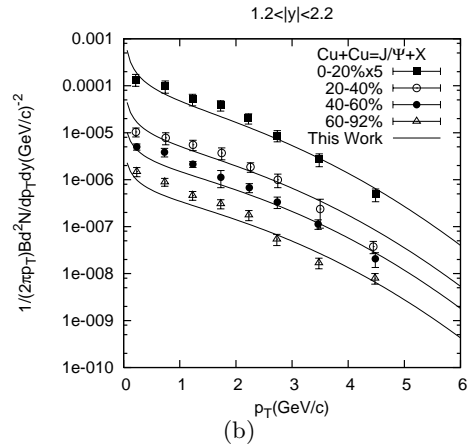
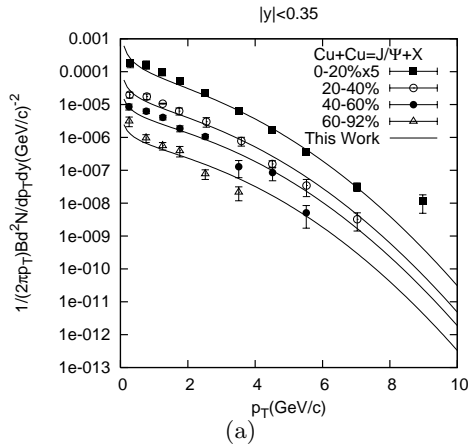


Figure 4: Transverse momenta spectra at (a)  $|y| < 0.35$  and (b)  $1.2 < |y| < 2.2$  for  $J/\Psi$  production in  $Cu + Cu$  collisions at  $\sqrt{s_{NN}} = 200 \text{ GeV}$ . The data are taken from [30]. The solid curves depict the SCM-based results.

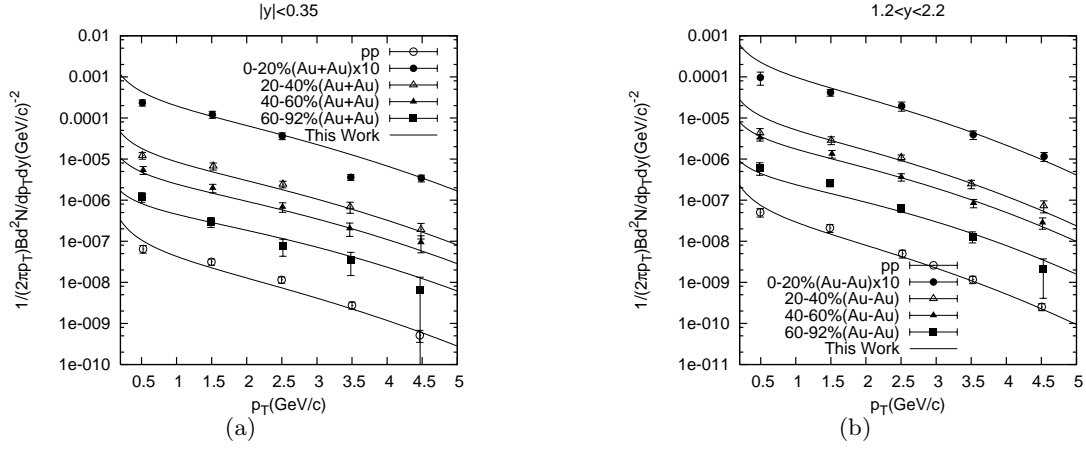


Figure 5: Invariant spectra as function of  $p_T$  for  $J/\Psi$  production in  $Au + Au$  collisions at  $\sqrt{s_{NN}} = 200\text{GeV}$  for (a)  $|y| < 0.35$  and (b)  $1.2 < |y| < 2.2$ . The data are taken from [31]. The solid lines show the SCM-based results.

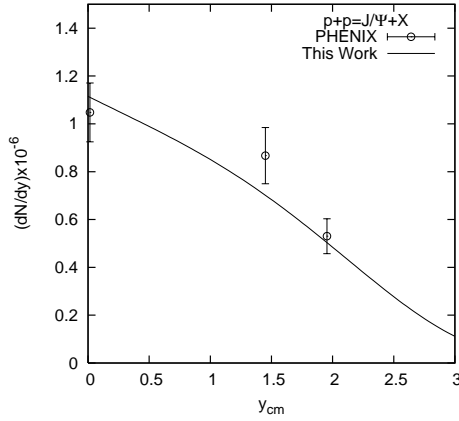


Figure 6: Plot of the rapidity distribution for  $J/\Psi$  production in proton-proton collisions at  $\sqrt{s_{NN}} = 200\text{GeV}$  as function of  $y$ . The data points are from [28]. The solid curves show the SCM-based results.

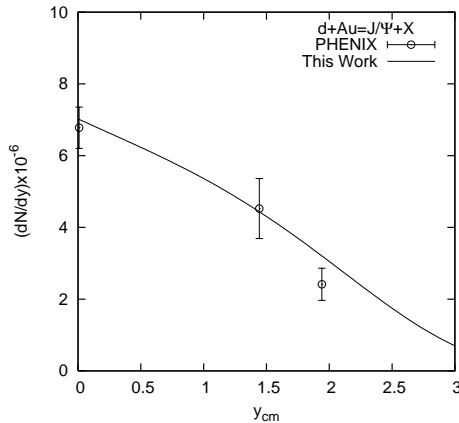


Figure 7: Rapidity distribution for  $J/\Psi$  production in  $d + Au$  collisions at  $\sqrt{s_{NN}} = 200\text{GeV}$ . The data points are from [28]. The solid curves show the SCM-based results.

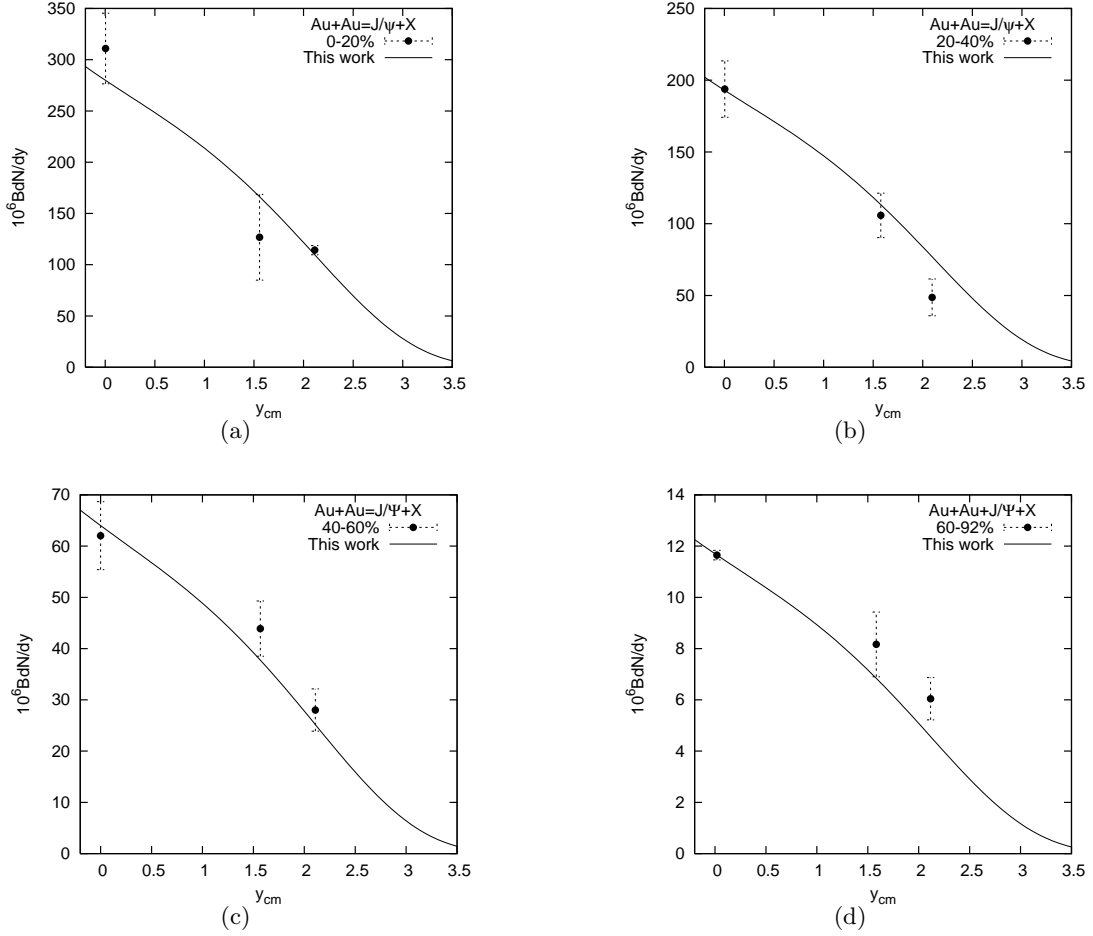


Figure 8: Plot of  $dn/dy$  vs.  $y_{cm}$ -values for  $Au + Au$  collisions at  $\sqrt{s_{NN}} = 200$  GeV for the centrality widths a) 0 – 20%, b) 20 – 40%, c) 40 – 60% and d) 60 – 92%. The data points are from [30]. The solid line shows the SCM-based results.

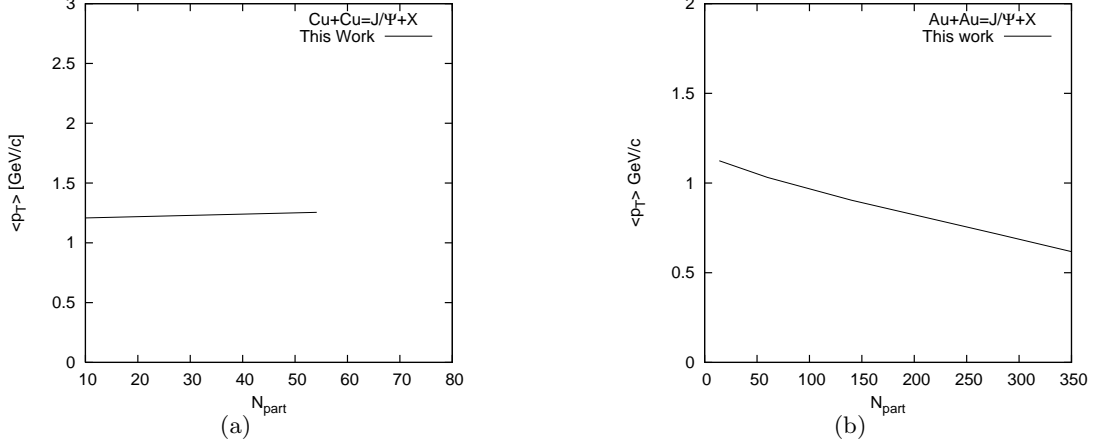


Figure 9:  $N_{part}$  vs. calculated results on  $\langle p_T \rangle^{J/\Psi}$  based on SCM for (a)  $Cu + Cu$  and for (b)  $Au + Au$ . The calculations are done on the basis of eqn.(4), Table 1 and Table 2. No experimental data on  $\langle p_T \rangle^{J/\Psi}$  are so far available. Calculated results are presented here in a predictive vein.

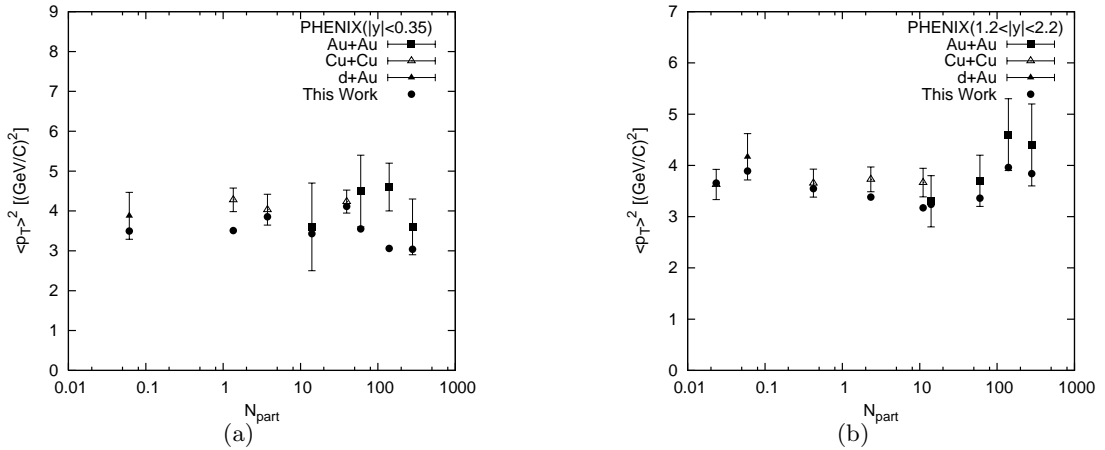


Figure 10: Plots on  $\langle p_T^2 \rangle$  versus  $N_{part}$  for  $J/\Psi$  production in  $d + Au$ ,  $Cu + Cu$  and  $Au + Au$  collision in (a) mid and (b) forward rapidities. The data points are taken from [28], [30] and [31] and the hollow circles in the Figure show the SCM-based results.

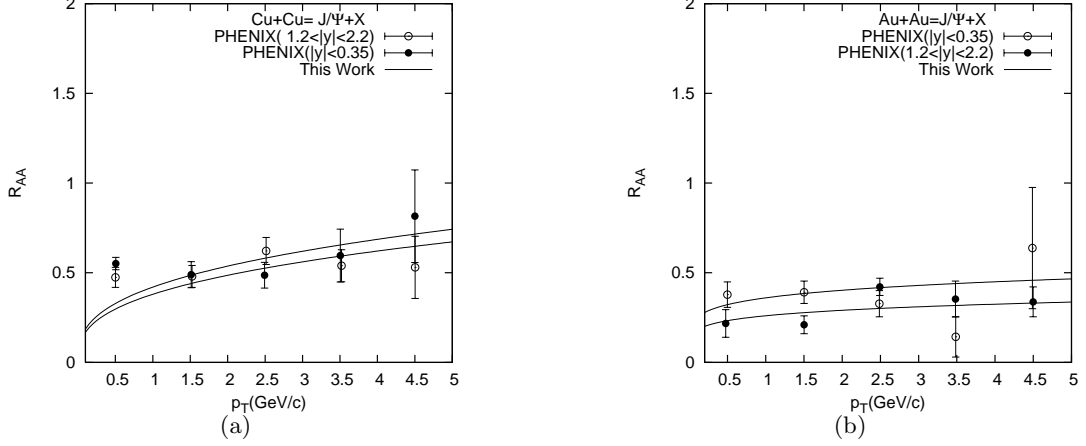


Figure 11: Plot of  $R_{AA}$  vs.  $p_T$ -values for 0 – 20% centrality in forward and mid-rapidities. The data points for  $Cu + Cu$  collisions (Fig. 8a) are taken from Ref.[30] while those for  $Au + Au$  collisions (Fig. 8b) are taken from Ref. [31] . The solid lines show the SCM-based results.

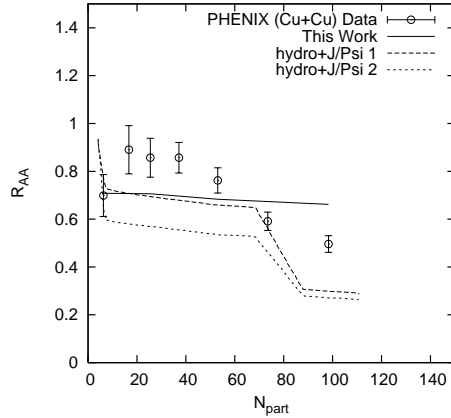


Figure 12: Nature of  $N_{part}$ -dependence of the nuclear modification factor (NMF) denoted by  $R_{AA}$  plots for  $Cu + Cu$  collisions at forward rapidity and at  $\sqrt{s_{NN}} = 200 GeV$ . The data are taken from Reference [30]. The SCM-based results are shown by the solid curved line in the Figure. The dashed curves show the predictions of the hydrodynamical model ('hydro+J/Psi') with (hydro+J/Psi1) and without (hydro+J/Psi2) nuclear absorption [37].

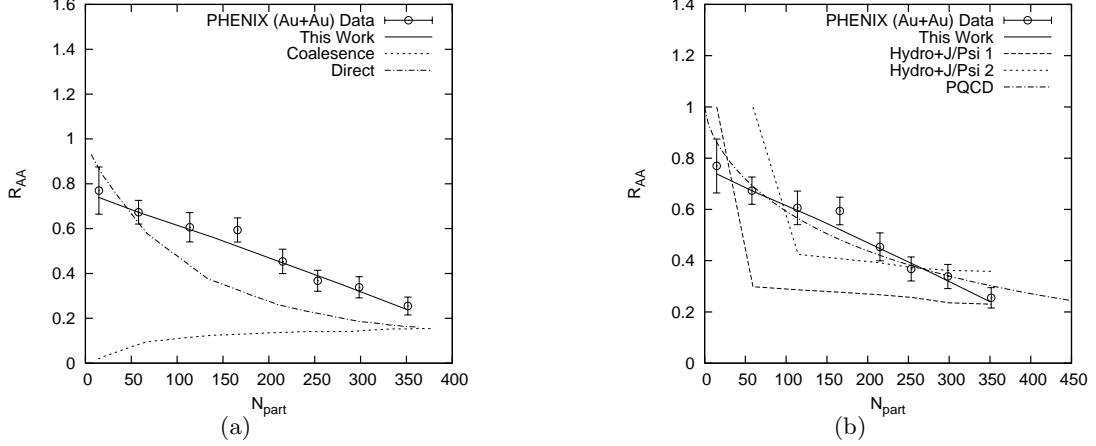


Figure 13: Nature of  $N_{part}$ -dependence of the nuclear modification factor (NMF) denoted by  $R_{AA}$  plots for  $Au + Au$  collisions at forward rapidity and at  $\sqrt{s_{NN}} = 200 \text{ GeV}$ . The data are taken from [31], [38]. The SCM-based result is compared with other theoretical results (a) Coalescence and Direct approaches [38] and (b) 'hydro+ $J/\Psi$ ' for  $T_{J/\Psi}/T_C = 1.2$  and  $1.4$  (hydro+ $J/\Psi$ 1, hydro+ $J/\Psi$ 2 respectively) [37], and PQCD from Ref. [39] in the Figures.

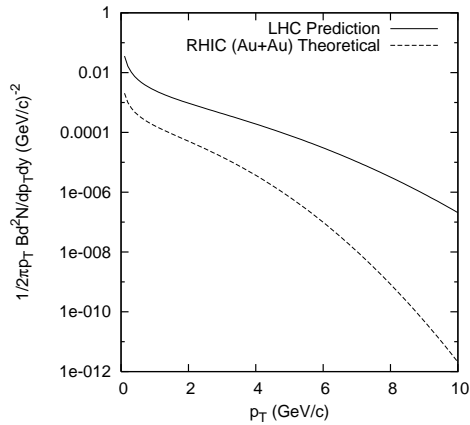


Figure 14: SCM-based predicted plot on  $J/\Psi$  production in the most central  $Pb + Pb$  collisions at  $\sqrt{s_{NN}} = 5500 \text{ GeV}$  i.e. at Large Hadron Collider (LHC) energy is shown by the solid curve. The dashed curve in the Figure represents our SCM-based plot for the most central collisions in  $Au + Au$  collisions at RHIC  $\sqrt{s_{NN}} = 200 \text{ GeV}$  energy.